

A wide-field K-band survey - II. Galaxy clustering

C.M. Baugh, J.P. Gardner, C.S. Frenk & R.M. Sharples

University of Durham, Department of Physics, Science Laboratories, South Road, Durham DH1 3LE

5 February 2008

ABSTRACT

We present the first measurement of the angular correlation function in a K -selected galaxy survey, from two fields covering almost 10 square degrees. The angular correlation function at small angles is well described by a $\theta^{-0.8}$ power law, as for optically selected samples. The clustering amplitude is reduced by a factor of ~ 4 between galaxies with $K < 15$ and a fainter magnitude slice with $15 < K < 16$. This allows us to place constraints upon the redshift distribution of the galaxies and their spatial correlation function. We find no clear evidence for a change in clustering amplitude when galaxies are selected by their observed $B - K$ colours.

Key words: surveys:galaxies: clustering - dark matter - large-scale structure of Universe - cosmology:observations - infrared:galaxies

1 INTRODUCTION

The measurement of angular correlations in optically selected samples of galaxies has been a useful probe of cosmological models and theories of galaxy formation. The shape of the angular correlation function, $w(\theta)$, on large scales measured in the APM Survey (Maddox *et al* 1990, 1996) showed that there is more structure in the galaxy distribution on large scales than is predicted by the standard Cold Dark Matter model. The scaling of the correlation amplitude with magnitude in faint samples has given some indication of the nature of faint blue galaxies (*e.g.* Efstathiou *et al.* 1991, Roche *et al.* 1993).

It is now possible to survey large areas of sky in the near-infrared K band. Measurement of the angular correlation function allows us to place constraints upon the shape of the redshift distribution of K -selected galaxies and on their spatial two point correlation function.

2 MEASURED CORRELATIONS

We have measured the clustering of galaxies in two fields imaged in the K band with a NICMOS3 detector and in the B , V and I bands using a 2048² CCD camera. Details of the image reduction can be found in Gardner *et al* (1996 in preparation). The star/galaxy separation for objects with $K < 15$, $I < 18$, $V < 19$ and $B < 20$ was carried out using a combination of image morphology and colour selection (Gardner 1995), and each galaxy identification was confirmed by eye. In the range $15 < K < 16$, the star/galaxy separation was performed using colour alone. The NEP field measures $1.97^\circ \times 2.58^\circ$, while the NGP field is rectangular with sides $6.91^\circ \times 0.66^\circ$. The NGP field contains a galaxy

cluster, so we have also estimated the angular correlations in this field with the ~ 0.7 square degrees containing the cluster removed. This effectively produces two disjoint regions which we designate NGP-CL.

The angular correlations were measured using three different estimators, which we shall refer to as the direct $w_d(\theta)$, Hamilton $w_h(\theta)$ (Hamilton 1993) and ensemble $w_e(\theta)$ estimators. In order to compute the direct and Hamilton estimates, 20000 points were put down at random within the survey regions. The ensemble estimator is calculated by dividing the fields into a grid of cells of side 0.02° . The form of the estimators is given by

$$w_d(\theta) = \frac{2N_R}{(N_G - 1)} \frac{\langle DD \rangle}{\langle DR \rangle} - 1 \quad (1)$$

$$w_h(\theta) = \frac{4\langle DD \rangle \langle RR \rangle}{\langle DR \rangle^2} - 1 \quad (2)$$

$$w_e(\theta) = \frac{\langle N_i N_j \rangle}{\langle N_i \rangle \langle N_j \rangle} - 1, \quad (3)$$

where N_G is the number of galaxies in the field that satisfy the specified magnitude limits and N_R is the number of random points. The angular brackets indicate an average over all pairs of points in the sample for the case of w_d and w_h , and an average over pairs of cells for the case of w_e , that are separated by angle $\theta \pm \delta\theta$. The quantities DD , DR and RR are the number of distinct data-data, data-random and random-random pairs at angular separation θ . The number of galaxies in cell i is given by N_i .

The direct estimator suffers from linear biases arising from spurious correlations between the survey window and the data and is restricted by the accuracy with which the mean density of galaxies is known (Hamilton 1993, Landy

Table 1. Measured angular correlations: The amplitude of a power law fit $w(\theta) = A\theta^{-0.8}$ is given along with the 2σ range. The final column gives the value of the integral constraint.

sample	field	number of galaxies	A	A (high)	A(low)	σ^2
$K < 15$	NGP	907	0.043	0.047	0.039	0.041
	NGP-CL	653	0.017	0.021	0.011	0.016
	NEP	675	0.035	0.039	0.029	0.042
$15 < K < 16$	NGP	2641	0.0096	0.0108	0.0088	0.0093
	NGP-CL	2144	0.0081	0.0093	0.0069	0.0081
	NEP	2122	0.0084	0.0098	0.0070	0.0102

& Szalay 1993). The Hamilton and ensemble estimators do not suffer from such a bias. The mean galaxy density is determined from the galaxy counts in each field, and so all the estimators will be biased low with respect to the true angular correlations by an amount

$$\sigma^2 \approx \frac{1}{\Omega^2} \int d\Omega_1 d\Omega_2 w_T(\theta_{12}), \quad (4)$$

where $w_T(\theta)$ is the true angular correlation function and Ω is the solid angle of the field (Groth & Peebles 1977). We estimate the size of this ‘missing variance’ or integral constraint by assuming that the true angular correlations are given by $w_T(\theta) = A\theta^{-0.8}$ and performing a Monte-Carlo integration of equation (4) over each field. The amplitude A is then set by fitting the measured correlation function on small angular scales to (Roche *et al* 1993):

$$w(\theta) = A\theta^{-0.8} - \sigma^2. \quad (5)$$

We have also estimated the magnitude of the integral constraint by calculating the variance in the number of galaxies found in mock versions of our fields drawn from a much larger simulated APM catalogue (Gaztañaga & Baugh 1996). The integral constraint found in this way is approximately 25% smaller, which indicates the error resulting from the assumption that $w(\theta)$ is a power law up to scales corresponding to the angular size of the field.

The angular correlations for galaxies with $K < 15$ are shown in Figure 1 for each field. Throughout this paper we plot the measured correlations plus the estimated value of the integral constraint, given in the final column of Table 1. We have measured $w(\theta)$ in logarithmic bins of width $\Delta \log \theta = 0.2$. The dotted line shows the angular correlation between the random points in each field and the data which biases the direct estimator. The dashed line shows the power-law correlation function given by a least squares fit to the measured correlations on scales of $0.005^\circ - 0.06^\circ$, as listed in Table 1 for the Hamilton estimator. The angular correlation function bins are not independent, so we quote the 2σ range in the fitted amplitude in columns 5 and 6 of Table 1. Errorbars are computed using $\delta w(\theta) = \sqrt{(1 + w(\theta))/\langle DD \rangle}$ (Hewitt 1982). This may underestimate the errors, so we plot the 2σ errors obtained from this formula. We have found that the 2σ errors computed in this way are comparable to the errors obtained with a bootstrap resampling of the data (Ling, Frenk & Barrow 1986).

The correlations in the NGP region rise above the power

law fitted to small scales in the angular range $0.06^\circ - 0.50^\circ$. The NEP field shows a deficit of pairs on these scales, compared with the fitted power law. This suggests that this field could be slightly underdense, as a break in $w(\theta)$ is not expected at $\theta < 1^\circ$ for $K < 15$; in the optical, this corresponds to a magnitude limit of approximately $B \approx 19$, and $w(\theta)$ is observed to be a power law until $\theta \approx 2^\circ$ (Maddox, Efstathiou & Sutherland 1996). The agreement between the values of $w(\theta)$ measured with the different estimators is impressive in the NEP and NGP fields. There are some discrepancies, however, between the estimators in the NGP-CL field due to the hole caused by omitting the cluster, which results in less reliable measurements of $w(\theta)$ in this field. From now on we shall plot only the angular correlation function obtained from the Hamilton estimator.

The angular correlation function in the $K < 15$ sample is compared with that in the deeper $15 < K < 16$ sample in Figure 2, where we have plotted $w_h(\theta)$, again with 2σ errors. The dashed lines show the power-law correlation function fitted to the measurements at small angles. There is a reduction in the amplitude of clustering by a factor of ~ 4 in the $15 < K < 16$ sample compared with the brighter sample. The correlations in the deeper NEP and NGP samples are better described by a power-law on all scales, suggesting that the sampling fluctuations which affect the brighter catalogue are no longer significant for $K < 16$.

Finally, we examine whether the clustering strength depends on galaxy colour. We find no consistent difference in the amplitude of $w(\theta)$ in each field when we split the $K < 16$ catalogue into ‘red’ and ‘blue’ galaxies at the median $B - K$ colour. Figure 3 compares the angular correlation function in the blue and red subsamples with the correlations for the whole $K < 16$ sample. In the NGP field, blue galaxies do appear to be more strongly clustered than both the red galaxies and the full sample. However, the angular correlations in this field are dominated by the presence of the cluster. In the region that contains the cluster, there are ~ 2 times more galaxies with blue colours compared with the number that have red colours. In the NEP field, the red galaxies appear to be more strongly clustered than the blue galaxies, in particular around $\log \theta \sim -0.6$.

3 INTERPRETATION

The angular correlation function is related to the spatial correlation function $\xi(r)$ and the redshift distribution of the

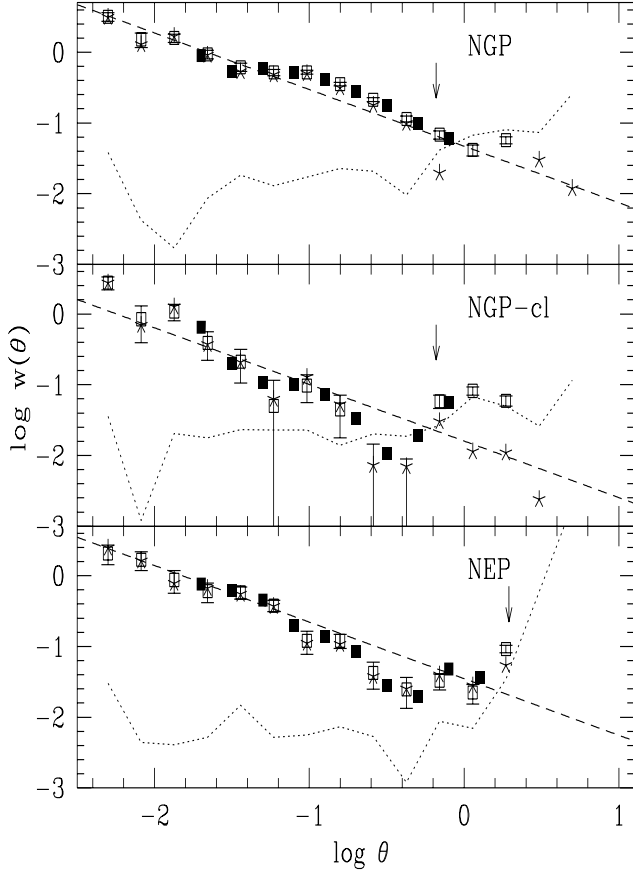


Figure 1. The measured angular correlation functions with the estimated integral constraint added for the NEP, NGP and NGP-CL regions for galaxies brighter than $K = 15$. The open squares show $w(\theta)$ calculated with the direct estimator, the filled squares with the ensemble estimator and the stars with Hamilton's estimator. The error bars on the direct estimator values are 2σ errors calculated as described in the text. The dashed line shows the power-law fitted to the measured $w(\theta)$ on small scales. The dotted line shows the random-galaxy correlations. The arrows indicate the smallest linear dimension of each field.

Table 2. The correlation length needed to reproduce the amplitude of clustering in the NEP field, for a range of theoretical redshift distributions and for two different cases of the evolution of clustering with redshift

redshift distribution	$K < 15$		$15 < K < 16$	
	r_0	ϵ	r_0	ϵ
optical fit	6.8	0.0	4.5	0.0
	6.3	-1.2	4.0	-1.2
passive evolution	7.5	0.0	6.1	0.0
	6.9	-1.2	5.2	-1.2
no evolution	6.3	0.0	4.3	0.0
	5.8	-1.2	3.8	-1.2

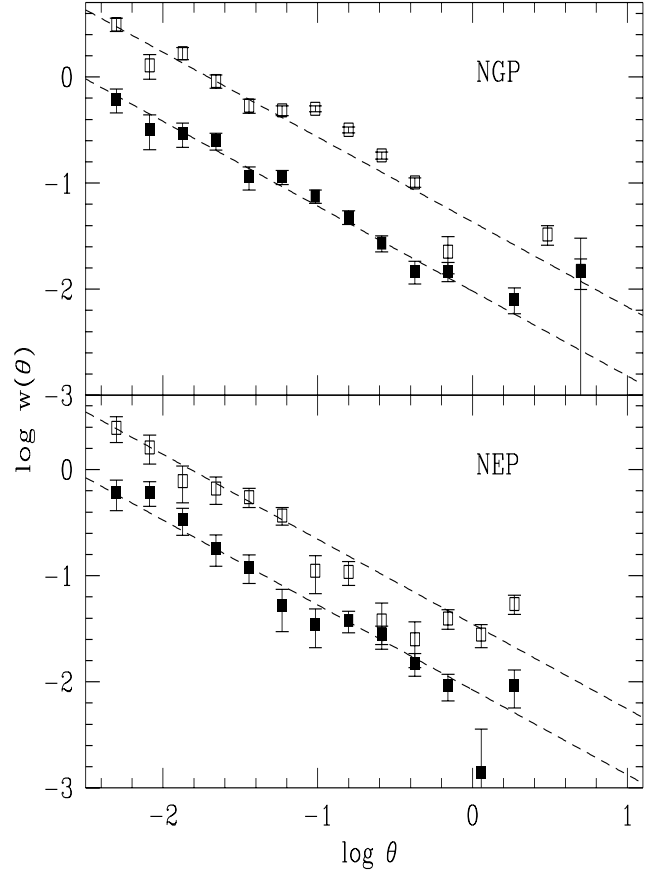


Figure 2. Angular correlation functions for galaxies with $K < 15$ (open squares) and $15 < K < 16$ (filled squares), with 2σ error bars calculated as described in the text. The dashed lines show the power law $w(\theta)$ fitted at small angles. The angular correlations are computed using the Hamilton estimator.

galaxies by Limber's equation (Peebles 1980, §56). On small scales, both $w(\theta)$ and $\xi(r)$ are measured to have power law forms (e.g. Davis & Peebles 1983, Maddox *et al* 1990, 1996, Baugh 1996) and Limber's equation can then be written in the form (Efstathiou *et al.* 1991):

$$w(\theta) = \sqrt{\pi} \frac{\Gamma((\gamma-1)/2)}{\Gamma(\gamma/2)} \frac{A}{\theta^{\gamma-1}} r_0^\gamma, \quad (6)$$

where

$$A = \int_0^\infty g(z) \left(\frac{dN}{dz} \right)^2 dz / \left[\int_0^\infty (dN/dz) dz \right]^2 \quad (7)$$

and

$$g(z) = (dz/dx) x^{1-\gamma} F(x) (1+z)^{-(3+\epsilon-\gamma)}, \quad (8)$$

where $F(x)$ depends upon the cosmology and is equal to unity for $\Omega = 1$. Here we have parameterised the redshift evolution of the spatial correlation function as

$$\xi(r, z) = \left(\frac{r_0}{r} \right)^\gamma (1+z)^{-(3+\epsilon)}. \quad (9)$$

If clustering is fixed in proper coordinates then $\epsilon = 0$. If the pattern of clustering is fixed instead in comoving coordinates, then $\epsilon \approx -1.2$ for $\gamma \approx 1.8$ (Efstathiou *et al* 1991).

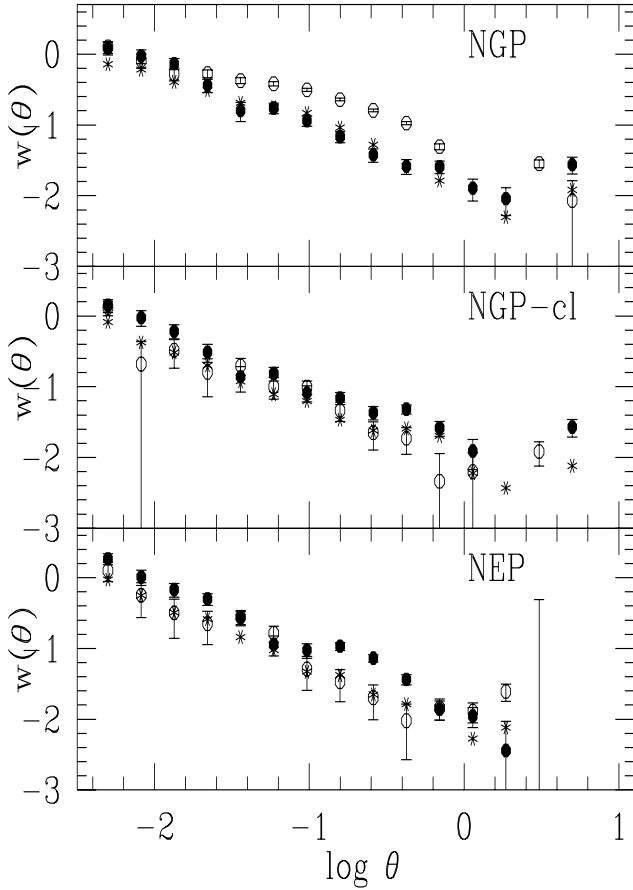


Figure 3. Angular correlation functions for galaxies selected by $B - K$ colour from the $K < 16$ sample. The stars show $w(\theta)$ for all galaxies. The filled circles show $w(\theta)$ for galaxies redder than the median $B - K$ colour, while open circles show $w(\theta)$ for galaxies bluer than the median $B - K$. The error bars are 2σ errors calculated as described in the text.

The redshift distribution of K -selected samples is less well determined than that of optical samples. In order to model the redshift distribution, we have combined redshifts from the Hawaii K -band Survey (Songaila *et al* 1994) and from Glazebrook *et al.* (1995), weighting each galaxy by the field area, sampling rate and redshift completeness fraction as described in Baugh & Efstathiou (1993). We have used the total K magnitudes listed in Table 3 of Songaila *et al* and the $20h^{-1}\text{kpc}$ metric aperture magnitudes from Table A1 of Glazebrook *et al.* Figure 4 shows the observed redshift distribution for several cuts in K magnitude. The solid curve shows the prediction of the parametric form adopted by Baugh & Efstathiou (1993) as a fit to the redshift distribution of optically selected galaxies

$$(dN/dz)dz = \frac{3\mathcal{N}(m)\Omega_s}{2z_c^3} z^2 \exp(-(z/z_c)^{3/2})dz, \quad (10)$$

where the median redshift is $z_m = 1.412z_c$. For the combined $13 < K < 15$ dataset, we find a median redshift of $z_m \sim 0.155$, whilst for the deeper slice $13 < K < 16$ we obtain $z_m \sim 0.175$. Also plotted are the predicted redshift distributions for ‘passive’ (dotted line) and ‘no evolution’ (dashed line) models constructed with the Bruzual

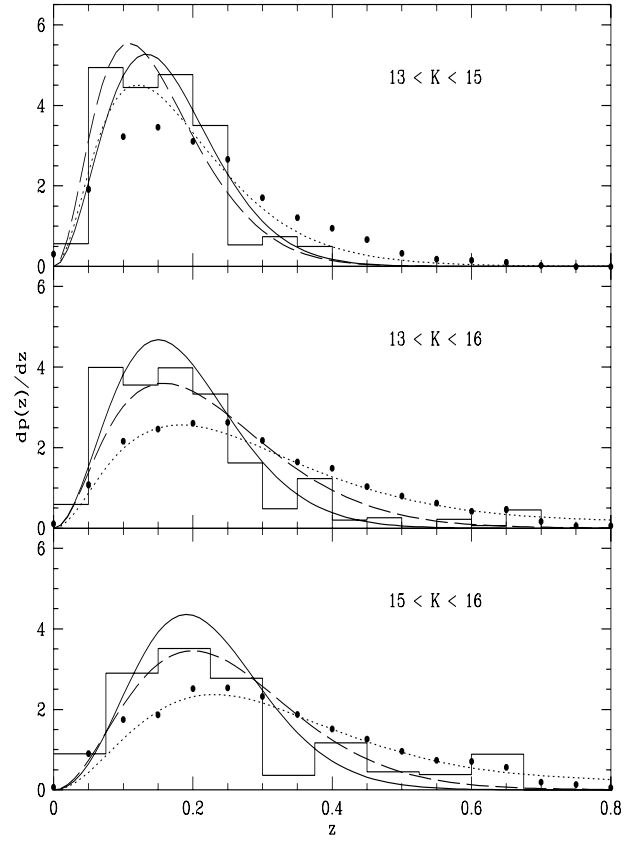


Figure 4. The histograms show the redshift distribution combined from the surveys of Songaila *et al.* (1994) and Glazebrook *et al.* (1995). The solid curve shows the parametric fit described in the text. The dashed curve shows the prediction of a no evolution model and the dotted curve shows a model with passive evolution. The circles show the predictions of the semi-analytic model for galaxy formation of Cole *et al* (1994).

and Charlot (1993, 1996 in preparation) spectral energy distributions described in Gardner *et al* (1996) and Gardner (1996). The circles show the predictions of the *ab initio* semi-analytic model for galaxy formation described by Cole *et al* (1994). The theoretical curves give reasonable fits to the combined dataset, except perhaps at higher redshifts, where in any case the observed redshift distribution is less well determined.

A further constraint on the form of the redshift distribution is the scaling of the amplitude of $w(\theta)$ with apparent magnitude between the $K < 15$ and $15 < K < 16$ samples. In Table 2 we find the values of the correlation length r_0 that reproduce the observed amplitude of the angular correlation function in the NEP field, for two specific cases of the evolution of clustering, $\epsilon = 0$ and $\epsilon = -1.2$. Local optically selected samples give $r_0 \sim 5h^{-1}\text{Mpc}$, though the real space spatial correlation function $\xi(r)$ has a shoulder feature between $4 < r < 25h^{-1}\text{Mpc}$ (Guzzo *et al* 1991, Baugh 1996, Ratcliffe *et al.* 1996), which complicates fitting a simple power law to $\xi(r)$.

4 SUMMARY

We have presented angular correlation functions, $w(\theta)$, for galaxies selected in the K -band over a large area of sky. We find that $w(\theta)$ is well fitted by a $\theta^{-0.8}$ power law on small angular scales, as observed for optically selected galaxies. There is a factor of ≈ 4 reduction in the amplitude of clustering for a faint magnitude slice, $15 < K < 16$, compared with galaxies with $K < 15$. This behaviour can be reproduced assuming the redshift distribution predicted by a simple no evolution model, if the correlation length of galaxies with a median redshift of $z \sim 0.23$ is around $4.3h^{-1}\text{Mpc}$ whilst for galaxies at a lower median redshift of $z \sim 0.13$, $r_0 \sim 6.3h^{-1}\text{Mpc}$, and clustering is fixed in proper coordinates. We find no consistent change in the strength of clustering in the different fields when galaxies are selected by their observed $B - K$ colours, but this does not rule out a dependence of clustering amplitude on colour in samples of higher median redshift (Landy *et al.* 1996).

The measured clustering contributes to the uncertainty in the number counts (Gardner *et al.* 1996) because different patches of sky contain different numbers of galaxies depending upon whether they are in high or low density regions. The integral constraint σ^2 gives an indication of the fractional variance in the number counts (see Peebles 1980 §36). Taking into account the fact that we have two widely separated fields, the rms variance at $K < 15$ is $\sigma_{rms} = 0.14$ whilst for $15 < K < 16$ $\sigma_{rms} = 0.07$. These values are upper limits, though tests with simulated catalogues that have the same clustering show that these numbers would be reduced by ~ 0.02 . The contribution to the variance in the counts from galaxy clustering is several times larger than that expected from Poisson statistics alone.

ACKNOWLEDGEMENTS

We would like to thank Esperanza Carrasco for assisting with the data collection. We acknowledge useful conversations with Richard Fong. This work was supported by a PPARC rolling grant for Extragalactic Astronomy and Cosmology at Durham.

REFERENCES

- Baugh, C.M., Efstathiou, G., 1993, MNRAS, 265, 145
 Baugh, C.M., 1996, MNRAS, 280, 267
 Bruzual, G.A., Charlot, S., 1993, ApJ, 405, 538
 Bruzual, G.A., Charlot, S., 1996, in preparation
 Cole, S., Aragon-Salamanca, A., Frenk, C.S., Navarro, J.F., Zepf, S.E., 1994, MNRAS, 271, 781
 Davis, M., Peebles, P.J.E., 1983, ApJ, 267, 465
 Efstathiou, G., Bernstein, G., Katz, N., Tyson, J., Guhathakurta, P., 1991, ApJ, 380, L47
 Gardner, J.P., 1995, ApJS, 98, 441
 Gardner, J.P., 1996, MNRAS, 279, 1157
 Gardner, J.P., Sharples, R.M., Carrasco, B.E., Frenk, C.S., 1996 MNRAS, submitted
 Gaztañaga, E., Baugh, C.M., 1996 in preparation
 Glazebrook, K., Peacock, J.A., Miller, L., Collins, C.A., 1995, MNRAS, 275, 169
 Groth, E.J., Peebles, P.J.E., 1977, ApJ, 217, 38
 Guzzo, L., Iovino, A., Chicarini, G., Giovanelli, R., Haynes, M.P., 1991, ApJ, 382, L5
 Hamilton, A.J.S., 1993, ApJ, 417, 19
 Hewitt, P.C., 1982, MNRAS, 201, 867
 Landy, S.D., Szalay, A.S., 1993, ApJ, 412, 64
 Landy, S.D., Szalay, A.S., Koo, D.C., 1996 ApJ, 460, 94
 Ling, E.N., Frenk, C.S., Barrow, J.D., 1986, MNRAS, 223, 21p
 Maddox, S.J., Efstathiou, G., Sutherland, W.J., Loveday, J., 1990, MNRAS, 242, 43p
 Maddox, S.J., Efstathiou, G., Sutherland, W.J., 1996, MNRAS, submitted
 Peebles, P.J.E., 1980 Large Scale Structure of the Universe, Princeton
 Ratcliffe, A., Shanks, T., Broadbent, A., Parker, Q.A., Watson, F.G., Oates, A.P., Fong, R., Collins, C.A., 1996, MNRAS, submitted
 Roche, N., Shanks, T., Metcalfe, N., Fong, R., 1993, MNRAS, 263, 360
 Songaila, A., Cowie, L.L., Hu, E.M., Gardner, J.P., 1994, ApJS, 94, 461